A PARAMETRIC STUDY OF AN ADAPTIVE LOAD-LIMITING RESTRAINT SYSTEM WITH WEIGHT SENSING CONSIDERATIONS

Jon van Poppel, M.Sc., P.E.
Amber Rath Stern, Ph.D., P.E.
David Fortenbaugh, Ph.D.
Grant Wilcox
Engineering Systems Inc.
United States

Paper Number 19-0057

ABSTRACT

The subject study provides an overview of several rear seat restraint configurations, with a focus on the restraint performance of a real-time adaptive (RTA) retractor system. The simulated RTA system assumes the integration of the TCJ Technology into the retractor. The near real-time response and high torque generation capabilities of the TCJ technology are briefly discussed and physical test data are shown in support. Simulations of both a conventional retractor and a 3kN LL retractor are carried out as well. The conventional retractor system is void of any specific energy management, other than the seatbelt stretch itself. Both the 3kN LL and the RTA systems are equipped with energy management functionalities. Simulations of the three restraint configurations are conducted in the MADYMO software with five different ATD models and six different crash pulses. The ATD models range from the HIII 6YO to the HIII 95th percentile male. The vehicle crash pulses originate from the NHTSA database for barrier impacts, with five pulses at the 35-mph severity level and one pulse at the 25-mph severity level. The MADYMO Control System modeling capabilities are relied upon to develop and implement the feedback control system for the RTA model. Seatbelt pay-out amounts and seatbelt pay-out rates are monitored during the simulated crash events. The sensor data are fed real-time into the RTA control system and real-time adaptive retractor seatbelt forces are thus generated. The research initially assumes direct occupant weight sensing is absent and later assesses that the RTA system can indeed function without this third input. A recommended load-limiting performance envelope for the RTA system is specified based on the simulation results. Data interpretation highlights the benefits of an RTA-type system for the full spectrum of modeled occupant sizes and weights, with an understanding that the smaller and more vulnerable occupants (elderly) tend to benefit most when restraint systems are more compliant, and yet able to prevent excessive seatbelt pay-outs for heavier occupants, without any significant detriment in injury numbers across the board. The noted improvements in the 25-mph simulation further bolster the broader benefit aspect, as a greater majority of occupant exposures occur at less than the 35-mph severity.

INTRODUCTION

The present research adds to recent reports and studies [1-5] that have investigated rear seat occupant safety systems. Contrary to front-seated locations, seatbelt systems are almost solely relied upon in rear-seated locations (for frontal impacts) because rear-seat locations cannot easily or very practically accommodate frontal airbag systems. Compared to front seat occupants, rear-seated passengers are also often of lighter weight (children). Further, the range of occupant sizes tends to be greater in rear-seated locations. Thus, rear seatbelt systems with different stiffness characteristics than those found in the current fleet might be desirable. Significant changes to rear seatbelt systems, however, cannot be easily realized under current regulations such as Federal Motor Vehicle Safety Standard (FMVSS) 209. Despite the FMVSS 209 requirements, the National Highway Traffic Safety Administration (NHTSA) recently sponsored a research project [6] that focused on broader rear restraint design possibilities, some of which edged on or went beyond FMVSS 209. A large segment of the NHTSA study included physical testing, but simulation results based on analyses with the MADYMO software were relied upon as well.

As in the NHTSA study, the work presented herein focused on tailoring the rear seat restraints performance envelope to a wider span of occupant weights, sizes, and types. The subject study also utilized the MADYMO software for baseline runs and alternative restraints design simulations. One of the alternative restraint designs was a real-time adaptive (RTA) seatbelt retractor system. The RTA system bases its performance characteristics on TCJ (Tailored Control Joint) technology, which has a fast response and high force generation capability [Appendix E]. As modeled, the RTA system represents a retractor in which the belt load adapts real-time to the dynamics of the

restraining event. Specifically, the RTA system is able to react to different occupant weights and sizes via a set of sensors and a control system whose definition is part of the work presented herein. The RTA control system ultimately operates based on the understanding that a heavy occupant will tend to yield a high seatbelt pay-out rate early in the crash pulse if the seatbelt force is too low, and the RTA system then drives the seatbelt force at the retractor to rise in such a case. Conversely, the seatbelt pay-out rate will typically be very low or zero for a lightweight occupant if the initial seatbelt force is too high, and the RTA system then drives the seatbelt force at the retractor to diminish in such a case, and thus increase the amount of seatbelt pay-out (increase of the light occupant ride-down distance).

Objectives of this study include addressing questions that relate to the investigation of real-world rear-seat restraints improvement opportunities, where frontal airbags are typically unavailable. Can an RTA system that responds as described above really be achieved without an occupant weight sensor signal from within the seat? What is an effective load range capability for the RTA retractor? Are the calculated injury values from the RTA model indeed tangibly lower across the collection of simulated ATD's? And also, how robust would such a system be, considering the unknown real-time nature of real-world crash pulses as they happen.

The RTA system is simulated together with other restraints configurations under a number of load conditions. Load conditions vary with combinations of different crash pulses ranging in severity from 25-mph to 35-mph and different anthropomorphic test devices (ATDs) ranging from the HIII 6YO to the HIII 95th percentile male. Results from the MADYMO simulations are then presented in the form of seatbelt performance data and injury metrics from the collection of ATDs.

BACKGROUND

The current research refers to some of the past work on rear seat restraints research, modeling and seatbelt system optimizations. Some of these studies have relied on the MADYMO or LS-Dyna simulation capabilities to investigate advanced and progressive rear seat restraints configurations, while others have relied on testing or a mix of the two approaches.

In a study conducted by Kawaguchi *et al.* [10], the proposed belt load controller was optimized with assistance of MADYMO modeling and concluded that a load limit value of 3.5 kN resulted in reduced injury values for all four of the modeled dummies. However, the overall results of the study suggested that lower load limits for small occupants and higher load limits for larger occupants would provide the best injury reduction potential when coupled with a pretensioner. A belt load limit of 2 kN and maximum pay-out length of 200 mm resulted in significantly reduced 6YO HIC and chest acceleration values when compared with the standard seatbelt model.

Hu *et al.* [11] used MADYMO, sled testing, and design optimization to examine whether a rear seating area designed for a 6-12 YO child would offer appropriate protection to other demographics including adults. Tradeoffs in occupant protection levels were observed with this approach. A design change that benefited one group sometimes reduced protection for another group. Hu *et al.* concluded the enhancement of rear seat occupant protection across all age groups for a single design required the use of adaptive or adjustable restraint systems.

Ravichandran [9] presented an optimization study conducted in the LS-Dyna explicit code environment with child dummies seated in rear positions. Seatbelt systems in the study were equipped with load-limiting levels ranging from 2 kN to 5 kN, stopper positions that varied from 0.8 to 1.5 torsion bar turns, and different pretensioner fire times. The study highlighted that the presented optimization method was an effective tool to identify an optimal restraint system to better protect second-row occupants.

A publication presented by Hong *et al.* [12] based several of their findings on 28 New Car Assessment Program (NCAP) tests in which a 10 YO child dummy was positioned in various rear seating positions. Nearly all 28 vehicles tested scored at least 4-stars for front seated occupants, while only a third of those vehicles maintained at least 4-stars for the rear seated occupants. The study also reported applicable belt loads and injury results curves.

Research on restraint system optimizations has also been conducted for first row seated locations [30 - 32]. Optimized systems typically owe their increased performance and injury reduction enhancements to appropriate

sensing technology, proper classification of the vehicle occupants, and/or ideal restraint systems modeling (systems that are not necessarily physical).

The current study operates similarly and proposes enhanced sensing technologies within the retractor, with active load-limiting functionalities based on a mechatronic system known as the TCJ technology. A TCJ-equipped system is characterized by a very fast response and a high force modulation capability – two features of significant importance to an RTA-type of retractor. The TCJ technology can generate an electrically controlled rotational friction force (effectively a torque) about the axis of rotation of a seatbelt retractor spool. Data from independent testing conducted at Intertek suggest a 15-millisecond response capability for multi-kN load changes, and minimal load variability either from the friction or from temperature variations (+/- 5% range of the target value). Belt loads from a TCJ-equipped retractor would typically vary around a pre-determined mid-point nominal load level (zero electrical input) from which the load can either increase or decrease, as needed. The mid-point load level for an initial exploration TCJ range of 1.5 kN to 6.0 kN, would be 3.75 kN, which is what was assumed in the current research (TCJ dimensions of approx. Ø65mm x L60 mm). A typical TCJ-retractor would have to be part of a control loop for the variation in the loads to be commanded (via a voltage input that is directly proportional to the generated restraint load). Appendix E provides reference information on the TCJ technology.

METHODOLOGY

The subject study investigated the performance of three seatbelt system configurations: a conventional belt (CB) system, a 3kN load-limited (3kN LL) belt system, and a real-time adaptive (RTA) restraint system. Both the 3kN LL and RTA systems incorporate what is known as an energy management (EM) system. Basic physics dictates that the dissipation of kinetic energy is directly dependent on a force time-history that is multiplied by a corresponding energy absorption distance (EAD) time-history. The objective of lowering the forces and maximizing the overall EAD of an occupant is then desirable, when possible, and EM systems are typically developed based on this strategy. For seatbelt cases, increased EADs come about by allowing seatbelt webbing to pay-out from the retractor via some form of tailored force that acts within the retractor as the seatbelt webbing spools out under the inertial loading of the occupant.

A wide variety of EM restraints technologies have been developed and produced over time, with most vehicles now equipped with some form of EM in their frontal restraint systems. There are currently limited possibilities for occupant-specific optimization of rear seat EM systems. The baseline CB case that was modeled herein is the most common implementation that meet FMVSS 209 guidelines [35], but it is void of any EM (aside from belt stretch properties). There are vehicles offering 6 kN LL-type belt systems at their rear-seated locations, and these systems also meet FMVSS 209. Such systems offer some EM benefits, but their performance is like CB systems for most occupants since lighter and mid-weight occupants will typically not generate the force needed to trigger the LL part of a 6kN LL system. To explore the patterns of LL effects for more occupant sizes, the present research incorporated the modeling of a 3kN LL EM system instead. A 3kN LL system represents a baseline technology to which the more complex RTA configuration can be compared. For the sake of reference, the RTA configuration, as modeled herein, operates both above and below the 3kN levels (with an initial 1.5 kN to 6.0 kN RTA load range capability).

The three retractor configurations in the current study were all subjected to the complete set of load case combinations stemming from the five different ATDs and six different crash pulses that were modeled. All six crash pulses originated from the NHTSA database. Table 1 offers a summary overview of the pulses, and Appendix A displays the pulse curves. The crash pulses were pulled from a small (B-segment) sedan, a C-segment sedan, a D-segment sedan, two medium SUVs, and an electric vehicle. All the crash pulses were 35-mph pulses, except for Pulse B, which was a 25-mph pulse.

Table 1.
Information on the selected NHTSA pulses.

Pulse Reference	Vehicle Type	NHTSA Test Impact Speed [mph]	Crash Type
A	Medium SUV	35	Fixed Barrier
B	Passenger Car (C-segment)	25	Fixed Barrier
C	Passenger Car (D-segment)	35	Fixed Barrier
D	Medium SUV	35	Fixed Barrier
E	Passenger Car (B-segment)	35	Fixed Barrier
F	Electric Vehicle (SUV-type)	35	Fixed Barrier

The five modeled ATDs consisted of the HIII 6YO, the Q10, the HIII 5th, the HIII 50th, and the HIII 95th. The parametric combination of six pulses, five ATDs, and three hardware configurations yielded a total of 90 MADYMO simulations.

Prior to generating restraint performance data and results from all the planned simulations, it was necessary to conduct a system identification process for the RTA system. The process started from the understanding that the RTA system could operate within an EM band that would range from 1.5 kN to 6.0 kN at the retractor, meaning that the RTA system would allow belt pay-out as soon as a 1.5 kN belt load was reached for some cases (light occupants or light pulse), but it could also "choose" to hold back any pay-out up to the 6.0 kN level (if needed, for heavier occupants), at which point pay-out would need to occur no matter what the energy profile of the crash event was. The system identification process continued as an iterative and non-automated process that considered the described EM load range for the RTA system (1.5 kN to 6.0 kN), the input for the assumed RTA sensor data sources, and the different load cases. An RTA system in which the belt load adapted real-time to the dynamics of the restraining event was thereby identified (i.e., the system adapts to the inertia of the occupant and to the severity of the crash pulse while maintaining favorable performance results).

Various simulation results from the RTA system in the subject study were analyzed and compared. RTA hardware results were first compared against the 3kN LL system to gauge the performance in terms of seatbelt pay-out amounts primarily. Shoulder belt load levels from the RTA system were also inspected and cross-compared in detail against the other systems. A review of injury numbers was conducted as well to evaluate the overall performance of the RTA system when compared against the most commonly implemented CB system. Reported injury metrics as generated from each of the modeled ATDs for all the simulated load cases included chest compression, chest acceleration, Head Injury Criterion (HIC), and Neck Injury Criterion (Nij) values. A brief sensitivity study was also carried out to evaluate the sensitivity of RTA injury results to variations in one of the key RTA modeling parameters.

MADYMO MODEL DESCRIPTION

The MADYMO software [37] is well-known for its ability to model automotive crash events incorporating ATDs, seatbelt systems, airbag systems, and the occupant environment itself. The software also offers Control Systems modeling capabilities, which were utilized herein as well. The build-up of the MADYMO simulations in the current study started from a simple and straightforward vehicle model that incorporated two front seats and a full rear seat bench. The right rear-seated location was the primary location of interest throughout this study. A three-point belt system was implemented at this location with one of three seatbelt retractor configurations:

1. the conventional belt (or CB) system, which is void of any EM beyond that of the belt stretch itself.
2. the previously described 3kN LL retractor system, with a static EM capability set at the 3kN force level.
3. the previously described RTA retractor system, equipped with an adaptive force generation system.

The modeling of the CB and 3kN LL retractor configurations was fairly straight forward. The RTA retractor modeling was more involved. It relied on real-time sensor signals to provide feedback about the retractor seatbelt pay-out and pay-out rate versus time. A MADYMO control system was thus implemented to collect these signals, process them, and command the seatbelt force level to the RTA retractor. Shown in Appendix D is a condensed view of the MADYMO syntax that was implemented for the RTA configuration, with each of the shown keyword lines having further syntax calls embedded within them. The formulations in MADYMO for the RTA system, and for the CB and 3kN LL systems, remained unmodified throughout the study, regardless of which ATD or pulse to which they were subjected.

MADYMO's pre-processor (XMADgic) was utilized to position a finite element model seatbelt around each modeled ATD. The HIII 6YO was positioned within a high back booster seat, whereas all the other ATDs were seated in a nominal position. In some simulations, ATDs occasionally interacted with the right front seatback via their extremities (light contacts, primarily with the hands and feet). In the modeled vehicle interior, there was enough space in all pulse cases to prevent the knees, even those of the HIII 95th percentile, from interacting with the seatback. Knee-to-seatback contacts might be likely in real-world situations, but it was preferred to initially isolate out this contact interaction in the subject simulations. Figure 1 shows schematic views of the RTA seatbelt system (a) prior to the crash, and (b) during the crash event. In more detail, Figure 1(b) illustrates the activated retractor, the seatbelt tension force, and the occupant belt loading which effects a Z(t) pay-out amount out of the retractor. The views shown in Figure 2 represent each of the five modeled ATDs, first shown at rest and then shown at the point where the maximum pay-out occurred out of the RTA retractor.

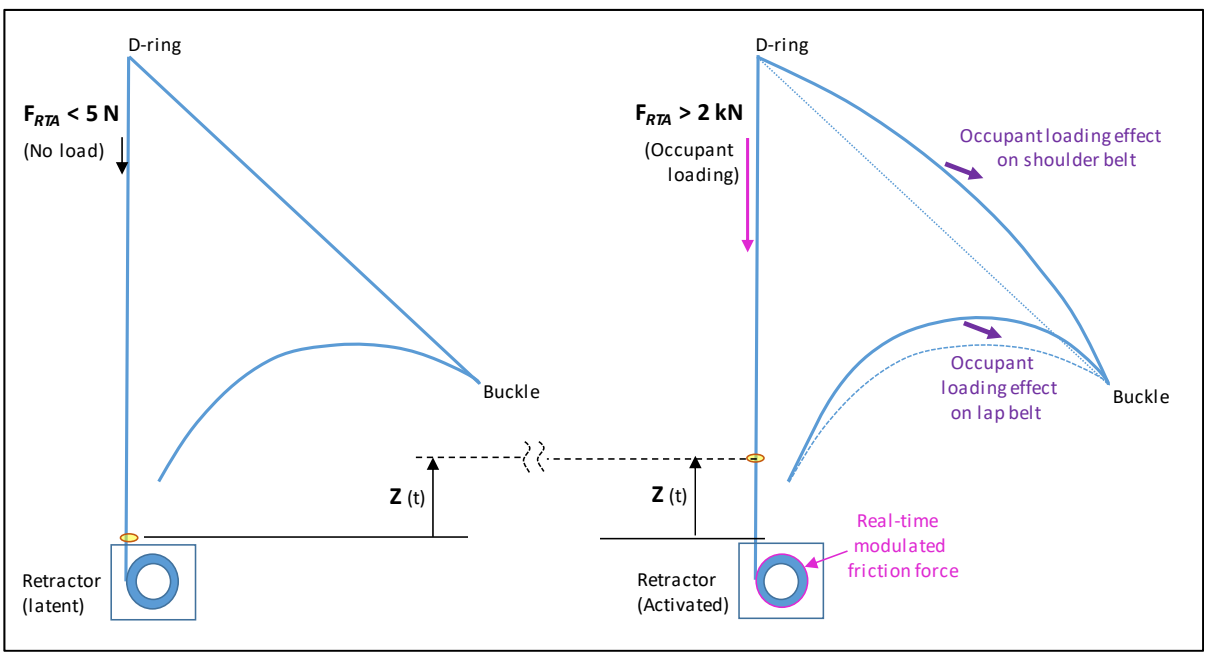

Pre-crash state of belt system
(a)

Snap-shot during a typical crash event
(b)

Figure 1. Diagrams of the RTA equipped 3-pt belt system.

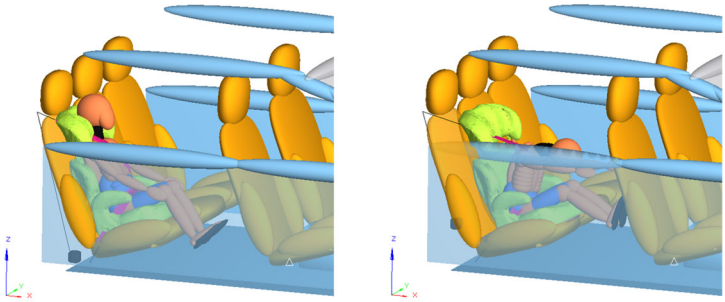

(a) HIII 6YO in high back booster seat

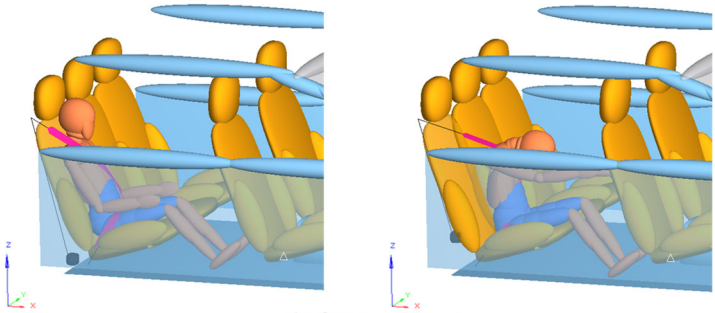

(b) Q10 in rear seat

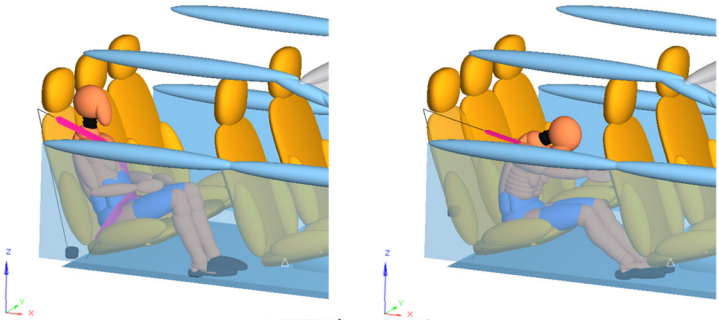

(c) HIII 5th percentile in rear seat

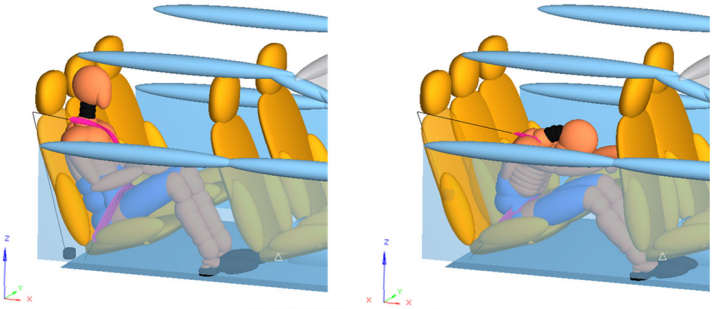

(d) HIII 50th percentile in rear seat

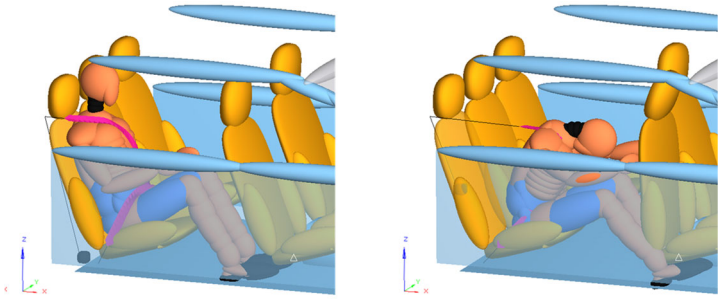

(e) HIII 95th percentile in rear seat

Figure 2. Sample Images from MADYMO simulations.

RESULTS

As discussed above, the simulations were carried out with three different seatbelt retractor configurations. Each hardware configuration yielded different seatbelt pay-out amounts and different seatbelt tension force time histories. An initial consideration of the retractor-specific data helps gauge their influence on the injury metrics. Recorded injury values from the different ATDs and crash pulses are reported in the Injury Metrics section provided below. The hardware results are reviewed first.

Hardware Results

Figures 3 and 4 provided below illustrate a sampling of the complete set of hardware simulation results. Both figures show only select curves from the HIII 50th percentile load case, for the purpose of identifying the trends.

Figure 3 displays retractor pay-out traces versus time for the 3kN LL and RTA configurations (there was no retractor pay-out for the CB case, and belt stretch effects were not accounted for in any of the pay-out data). The general trend was that for less forceful cases such as Pulse C (as marked in Figure 3), the RTA system tended to yield increased pay-out amounts over the 3kN LL case and vice versa for the more forceful cases, such as Pulse E (as marked in Figure 3 as well), in which the RTA system tended to withhold pay-out amounts over the 3kN LL case. Refer to Appendix B for the full collection of belt pay-out graphs for all ATDs and load cases.

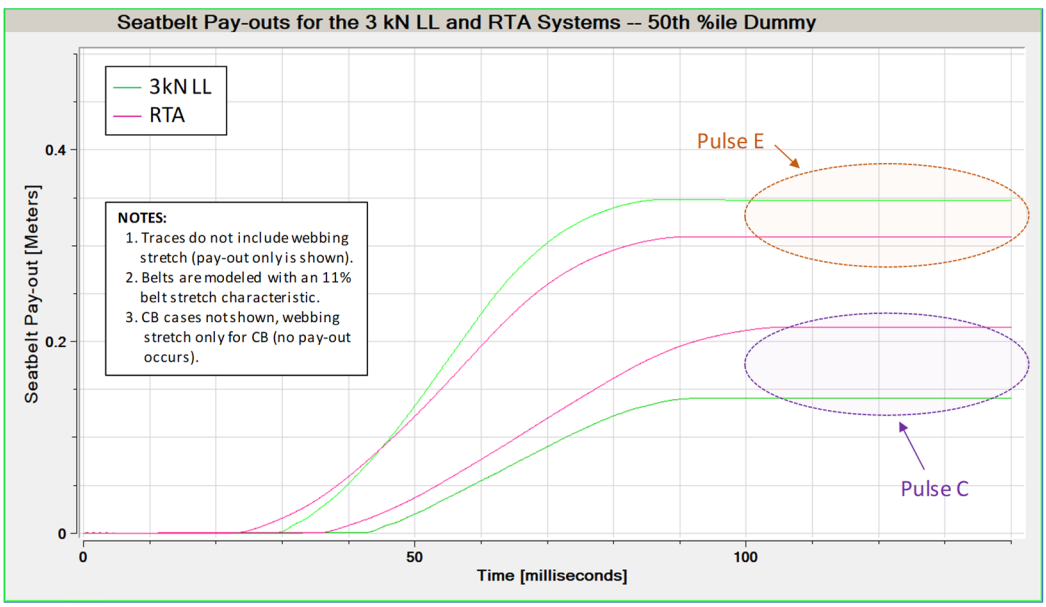

Figure 3. Webbing pay-outs out of retractor (sample results) – HIII 50th %ile ATD simulations.

Figure 4 is a sample graph of the shoulder belt load versus time traces, again for the HIII 50th percentile ATD only. As with Figure 3, shoulder belt load traces are shown only for two sample pulses (Pulses C and E). The contrast in Figure 4 is between result traces for the CB and RTA configurations primarily, since the 3kN LL hardware configuration always peaked out at approximately the same shoulder belt load level (being a 3kN LL configuration at the retractor, it peaked and remained steady at approximately 4 kN after belt passage over the D-ring for all cases). The CB simulations peaked at approximately 7 kN and 11 kN (Pulses C and E, respectively), and the RTA system peaked at approximately 3.6 kN and 6.2 kN for the same two Pulses C and E, respectively. Refer to Appendix C for a collection of shoulder belt load graphs for several ATD and load cases (lower severity Pulses B and C are omitted in the graphs in Appendix C only for the purpose of readability – Pulse C in Figure 4 provides a sense of the pattern for a lower severity pulse).

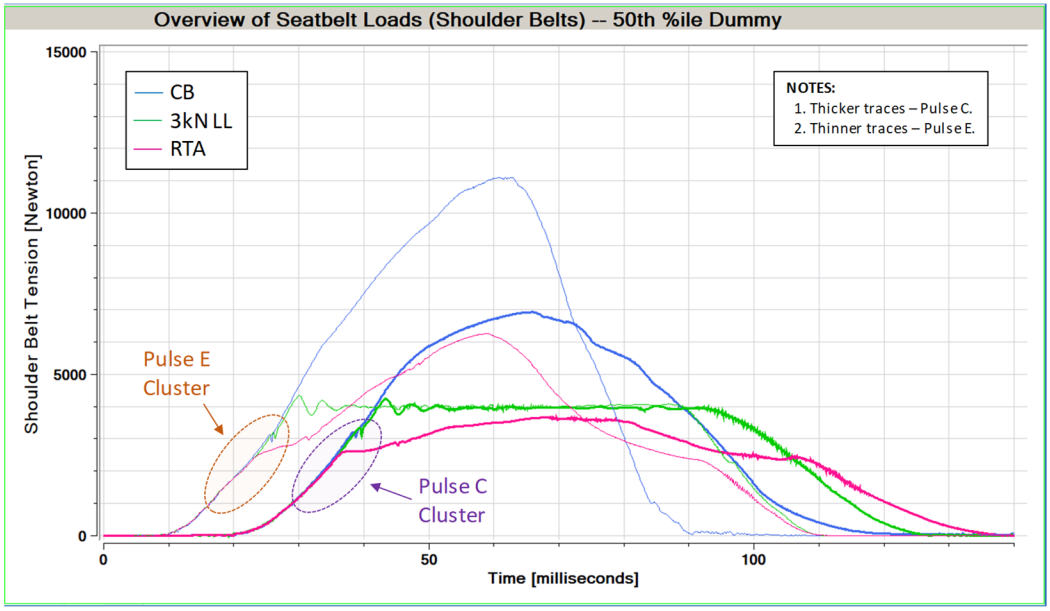

Figure 4. Seatbelt load traces (sample results) – HIII 50th %ile ATD simulations.

Injury Metrics Results

Injury metric results for the five dummies that were simulated in each of the parametric restraint and pulse conditions were analyzed. Four figures are provided below, each consisting of five histogram graphs (one per ATD -- see Figures 5 to 8). Six clusters of data appear within each histogram – one cluster per crash pulse. The data clusters are graphed in order of reducing crash pulse severity (from left to right). Detailed crash pulse information appears in Table 1 and traces are shown in Appendix A. Pulse E was the most severe of the collection of modeled pulses. Injury data are shown first in the form of chest compression values in Figure 5. Shown adjacent to the chest compression results are the chest acceleration results in Figure 6. Next, shown in Figures 7 and 8, are the HIC_{15} and N_{ij} values, respectively.

Results from the sensitivity study on RTA modeling parameters are presented as well, but they appear further below in the Discussion section. The sensitivity study is itself dependent on some of the findings brought forth in the Discussion section, and results for the sensitivity study are discussed then.

DISCUSSION

As mentioned previously, one objective of the subject study was to evaluate the likelihood of success, or feasibility, of an RTA system that is initially blind to the inertia of the occupant. As modeled herein, the RTA system thus relied on data originating only from two (admittedly assumed) sensors that measured the real-time seatbelt pay-out, $Z(t)$, and pay-out rate, $\dot{Z}(t)$, versus time. The RTA system was void of a seat-integrated weight sensor of any type. Upon examining Figures 5 through 8 and comparing the RTA data to the CB data, it transpires that RTA injury results improved in most instances, and often by a notable step, over CB results. Nij values did increase for the HIII 95th, but they remained below 1.0, while all the recorded high HIC values in the CB case for the HIII 95th were brought down to below 700 in all cases for the RTA configuration. Based on an overall review of injury numbers, it appears feasible therefore for an RTA system, as configured herein, to be successful.

Improved injury numbers as observed for the RTA system over results from the CB simulations should not, however, come at the expense of excessive seatbelt pay-out amounts. The more energetic simulations (HIII 95th percentile) for the 3kN LL case occasionally generated pay-out amounts that went beyond 400 mm. By contrast, the HIII 95th percentile pay-out results for the RTA system remained below 400 mm (maximum values of approximately 350 to 370 mm). Therefore, as it was configured herein, the RTA system appeared to capture the spirit of FMVSS 209, which allows up to 508 mm to be added to the belt system under high loading conditions (including belt stretch). As mentioned previously, belt stretch was not included in any of the reported seatbelt pay-out amounts in the subject study, and simulations were run with an 11% belt stretch characteristic.

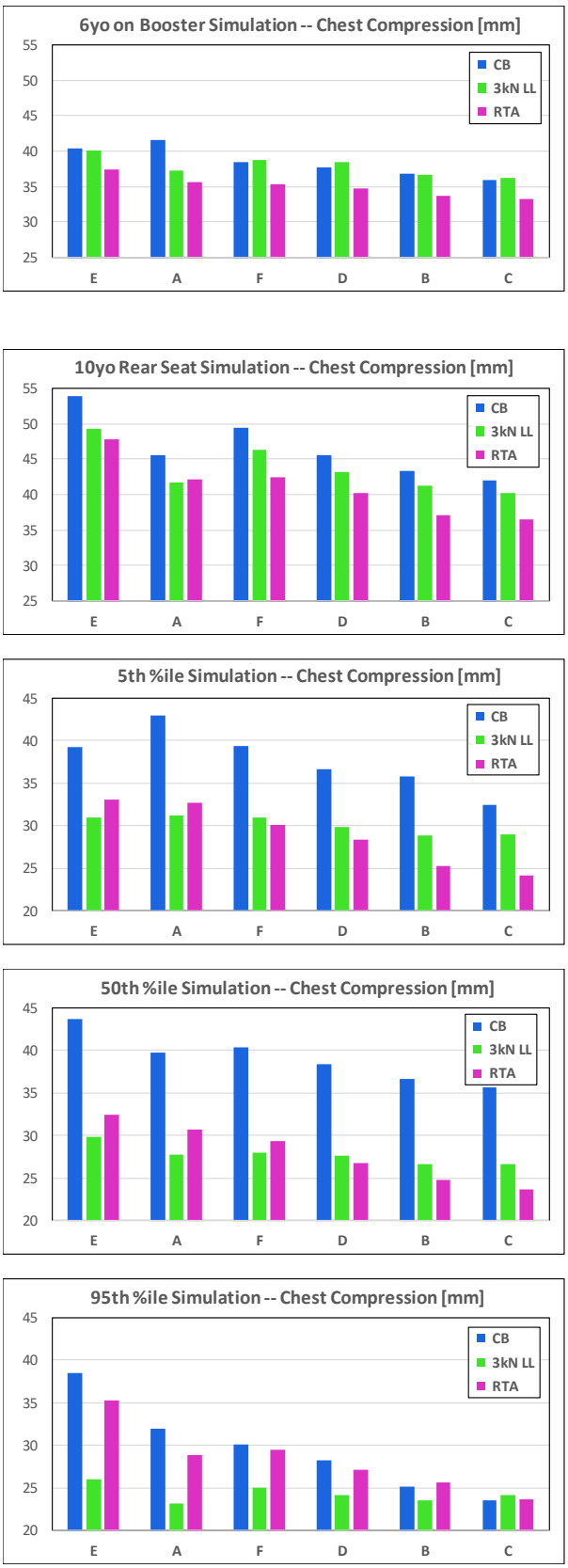

Figure 5. Chest Compressions – All load cases.

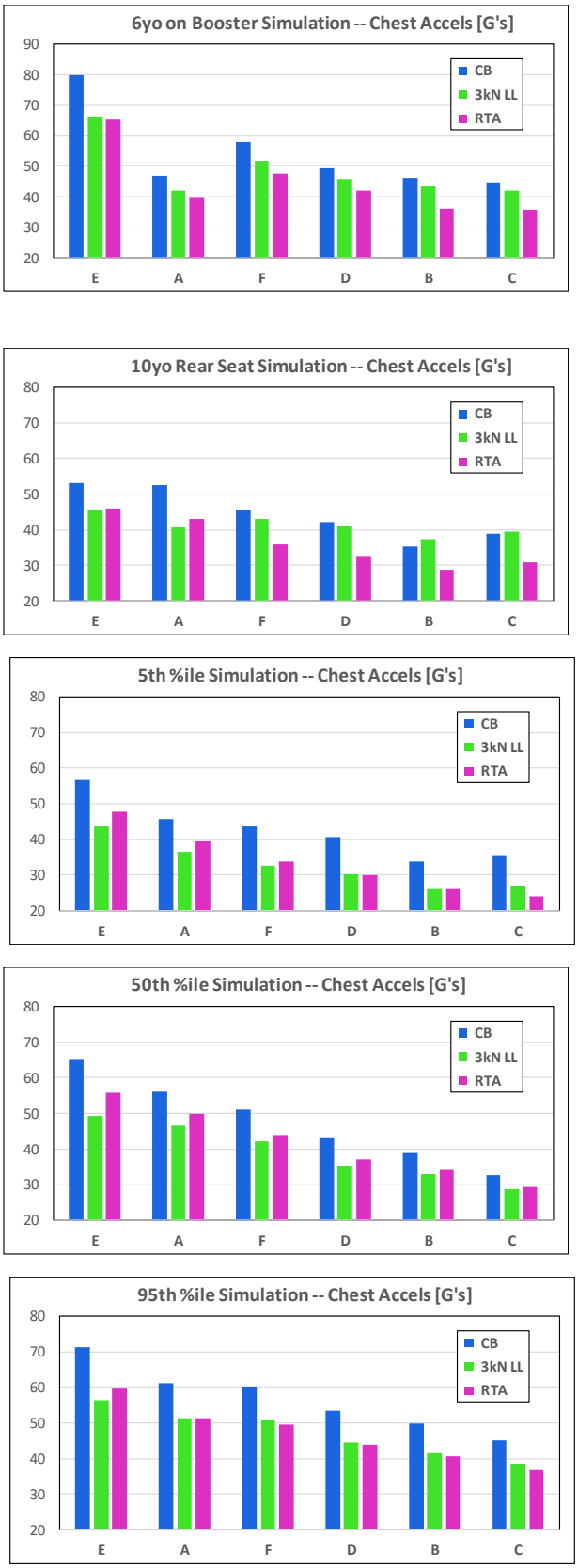

Figure 6. Chest Accelerations – All load cases.

Figure 7. HIC_{15} Values – All load cases.

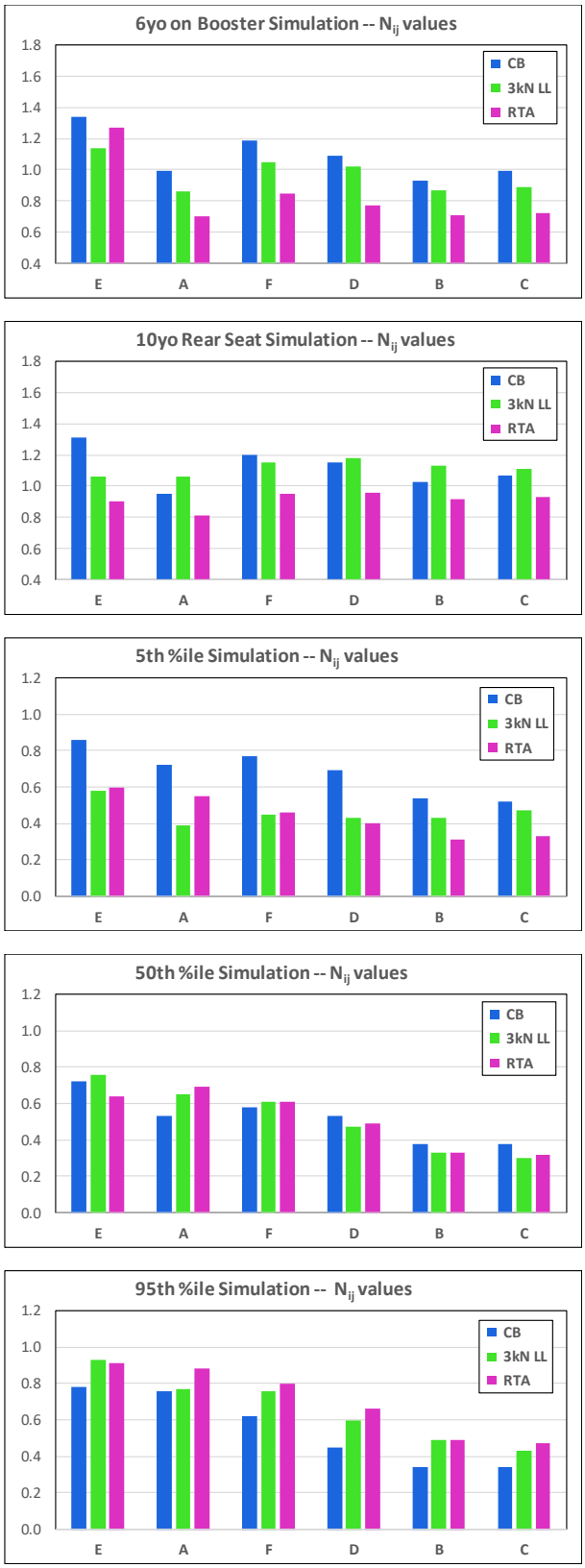

Figure 8. N_{ij} Values – All load cases.

Injury result trends and seatbelt performance data for the less energetic 25-mph crash severity (Pulse B) are of note as well. All four injury categories showed improvements in the RTA case for all the lower inertia ATDs. The significance of this observation is about the potential benefits for a wider segment of the population, with a focus on children and other more vulnerable occupants (elderly). While nominally tested ATDs already scored well with the CB system (5th and 50th ATD results are well below injury assessment reference values) in the 25-mph simulation, the RTA system continues to improve on those results. The potential real-world benefits associated with these improved responses are two-fold. First, a greater majority of crashes that occur on the roadways are indeed of delta-V's well below 35 mph [36]. Notable improvements in injury numbers for any crash severity lower than 35 mph apply then to a much greater number of real-world cases. This then increases the occupant exposures to improvements in real-world crashes. Secondly, the category of occupants that includes vulnerable populations such as the elderly and lighter weight individuals will benefit from the improved and adaptive performance of an RTA-type of system, while there was no appreciable adverse effects noted on the overall for the larger vehicle occupants.

As far as the system identification process is concerned, the understanding is that the RTA control system assimilates both the $Z(t)$ and $\dot{Z}(t)$ real-time information, and it then generates the adequate amount of retractor tension force, $F_{RTA}(t)$, that is required to manage the real-time dynamics of the restraining event. The system identification finding here is that the function, shown below in Equation (2), is one that in fact relates the two measured $Z(t)$ and $\dot{Z}(t)$ values to the retractor tension force, $F_{RTA}(t)$:

$$\mathbf{F_{RTA}(t) = f\left(Z(t),\ \dot{Z}(t)\right)} \qquad \text{(Equation 1)}$$

$$\mathbf{= 2000 + k_1 * Z(t) * \dot{Z}(t) - k_2 * \left[\ 1 - k_3 * \dot{Z}(t)^2\ \right] + k_4} \qquad \text{(Equation 2)}$$

Equation (2) is a function derived from iterative MADYMO simulations in which one control module after another was added into the complete sequence of control system modules. The stack of modules, when all combined after satisfactory results were generated, eventually distilled down to the formulation shown above in Equation (2).

The constant "2000" in Equation (2) has a physical meaning in that it is reflective of the lower end load-limited operation range of the RTA retractor (2.0 kN). The shoulder belt data from the complete set of RTA simulations (Appendix C) indicated a "step" (a visible transition) in the data traces at approximately 2.6 kN. The difference between the 2.0 kN value (at the retractor) and 2.6 kN (shoulder belt load) was due to the modeled friction at the D-ring. The 2.6 kN level in the shoulder belt was the point at which the traces either ceased to increase rapidly for lightweight occupants, or it was the point where the traces continued to rise, albeit at a visibly different rate, for larger occupants and/or more aggressive pulses.

A sensitivity analysis was also conducted on the first constant parameter in Equation (2). The finding was that lowering the "2000" (or 2.0 kN) that is currently assigned resulted in undesirable trade-offs. On the basis of injury values provided in Figure 9(a) for the low-end inertia HIII 6YO and in Figure 9(b) for the high-end inertia HIII 95th ATDs, dialing the constant in Equation (2) back to "1500" yielded non-negligible increases (for higher severity pulses) in both the HIC and N_{ij} values of the HIII 6 YO, and no discernable improvements in chest compression and chest accelerations for the same HIII 6YOA were noted. A similar comparison is shown in Figure 10 for seatbelt pay-out amounts, where the "1500" setting was shown to generate excessive pay-out amounts for the higher inertia HIII 95th percentile ATD, with pay-out values either exceeding or coming close to 400 mm in many of the simulations. Thus, the overall preference was to retain a value of "2000" (or 2.0 kN for the lower LL threshold in the RTA system) for the first constant term in Equation (2).

The latter finding bolsters the outcome for the lower RTA range setting to remain at 2.0 kN. On the high-end of the range, despite an original set limit of 6.0 kN for the RTA system, none of the RTA simulations truly approached that value – the maximum observed was 5.3 kN (or 6.9 kN at the shoulder belt). A working RTA load range at the retractor of 2.0 kN to 5.3 kN appears reasonable then, for the collection of load cases reviewed herein. The 2.0 kN to 5.3 kN is a much narrower band than the initially specified 1.5 kN to 6.0 kN. The finding of a narrower band is a favorable outcome in that it diminishes the complexity and functional design requirements of an RTA-type of system, which then likely reduces development and further downstream costs. The updated range of 2.0 kN to 5.3 kN thus became the working range for the RTA simulations that generated all the results shown in Figures 3 through 8 (and Appendices B and C).

(a) *(b)*

Figure 9. Sensitivity analysis -- Injury values between two RTA settings.

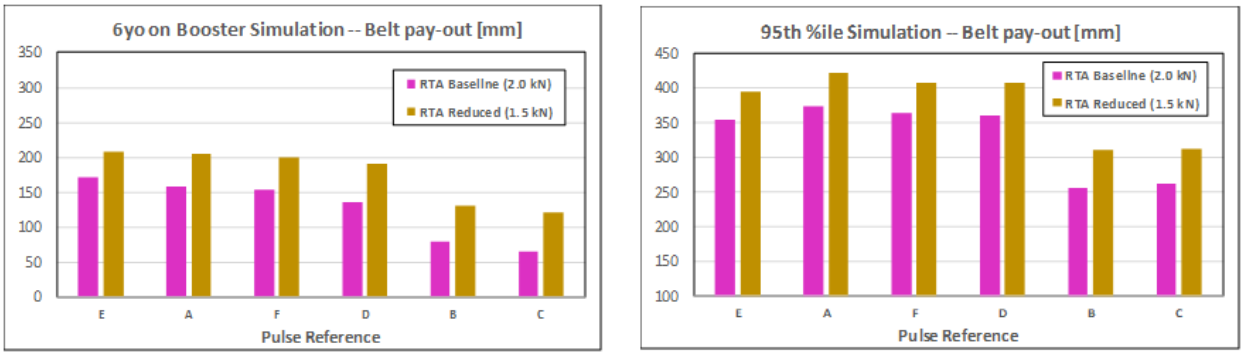

(a) *(b)*

Figure 10. Sensitivity analysis -- seatbelt pay-outs between two RTA settings and the 6YO(a) and HIII 95th(b).

CONCLUSIONS

Upon engaging into the subject research effort on adaptive restraints, it was unknown if an RTA retractor with the intended and ambitious functionalities could even be modeled successfully. An initial finding from this study is that the MADYMO software is able to model such an RTA-type of retractor, even with its native and somewhat limited MADYMO Control Systems commands (the coupling of MADYMO with MATLAB for more complex applications was not a necessary option herein). Also emerging as a finding from the subject research is that an overall and satisfactory restraint performance appears to be achievable with an RTA system that operates within a load-limited range spanning from 2.0 kN to 5.3 kN at the retractor. The overall RTA restraint performance was deemed satisfactory based on collected injury numbers from numerous simulation load cases, and on the basis that excessive seatbelt pay-out amounts were not observed, even for the higher inertia HIII 95th percentile ATD.

The RTA system was successfully simulated without relying on a weight sensing feature in the occupant seat. The RTA configuration instead assumed feedback for its control loop from both a seatbelt pay-out sensor and a pay-out rate sensor. The occupant inertia was therefore estimated from the instantaneous dynamics of the restraints event, and the RTA system reacted adequately thanks to the reversible and continuously variable capabilities of the TCJ technology, which the simulated RTA system was essentially representing.

The subject research is ultimately a feasibility study. Future work would be to focus on the details of the control system itself, such as sensor resolution characteristics, sensor response times, electronic actuation response times, and other possible component-specific dynamics. It remains to be seen, as such, how much effective lag time the RTA system could withstand and yet remain successful and useful. Also, the influence of the presence of a pretensioner remains to be investigated. Additional analyses related to specific injury potential, passenger interaction with the front seats of smaller vehicles, and crash pulses that are not primarily frontal in nature are areas of future focus as well. Despite the work that remains on several fronts, the subject research provided an initial concept validation for a physically realizable advanced restraint system that would likely benefit the more vulnerable vehicle occupants, such as children and elderly individuals, without generating any significant adverse effects for the typical adult weights and sizes upon which conventional restraint systems designs are usually based.

REFERENCES

[1] Vasilash, G. S. (2014, May 30) *Safety in the rear seat*. Automotive Design & Production. Retrieved from www.adandp.cm.

[2] Sahraei, E., Digges, K. and Marzougui, D. (2010). *Reduced Protection for Belted Occupants in Rear Seats Relative to Front Seats of New Model Year Vehicles*. In: 54th Annual Scientific Conference. Las Vegas, Nevada: Association for the Advancement of Automotive Medicine, pp.149-158.

[3] Sahraei, E., Soudbakhsh, D., and Digges, K. (2009) *Protection of Rear Seat Occupants in Frontal Crashes, Controlling for Occupant and Crash Characteristics*. Stapp Car Crash Journal, 53, pp. 75-91. Paper No. 2009-22-0003.

[4] Hu, J. (2016) *Surviving a Crash in Rear Seats: Addressing the Needs from a Diverse Population*. UMTRI, Transportation Research Institute University of Michigan, MADYMO User Meeting 2016.

[5] Dinh-Zarr, T. B. (2016, April 26) *Workshop: Rear Seat Safety in Passenger Vehicles*., National Transportation Safety Board, Washington, D.C.

[6] Hu, J., Rupp, J., Reed, M. P., Fischer, K., Lange, P., & Adler, A. (2016, March). *Rear seat restraint optimization considering the needs from a diverse population* (Report No. DOT HS 812 248). Washington, DC: National Highway Traffic Safety Administration.

[7] Hu, J., Reed, M., Rupp, J., Fischer, K., Lange, P. and Adler, A. (2017). *Optimizing Seat Belt and Airbag Designs for Rear Seat Occupant Protection in Frontal Crashes*. SAE International, SAE Technical Papers, 61st SAE Stapp Car Crash Conference, November 13-15, 2017, 61, 67-100.

[8] Wang, Y., Bai, Z., Cao, L., Reed, M., Fischer, K., Adler, A. and Hu, J. (2015). *A Simulation Study on the Efficacy of Advanced Belt Restraints to Mitigate the Effects of Obesity for Rear-Seat Occupant Protection in Frontal Crashes*. Traffic Injury Prevention, 16, S75–S83. DOI: 10.1080/15389588.2015.1010722.

[9] Ravichandran, V. (2018). *Multi-Objective Optimization for Vehicle Second Row Restraint System Considering Various Occupant Sizes and NCAP Requirements*. FISITA, 37th FISITA World Automotive Congress, October 2-5, 2018.

[10] Kawaguchi, K., Kaneko, N., Iwamoto, T., Fukushima, M., Abe, A., and Ogawa, S. (2003). *Optimized Restraint Systems for Various-Sized Rear Seat Occupants in Frontal Crash*. SAE International, SAE Technical Papers, SAE World Congress, March 3-6, 2003.

[11] Hu, J., Wu, J., Klinich, K., Reed, M., Rupp, J., and Cao. J. (2013). *Optimizing the Rear Seat Environment for Older Children, Adults and Infants*. Traffic Injury Prevention, 14: sup1, S13-S22, DOI: 10.1080/15389588.2013.796043.

[12] Hong, S. W., Park, C., Morgan, R., and Kan, C. (2008). *A Study of the Rear Seat Occupant Safety using a 10-Year-Old Child Dummy in the New Car Assessment Program*. SAE International, SAE Technical papers, Paper No. 2008-01-0511.

[13] Kent, R., Forman, J., Parent, D., and Kuppa, S. (2007). *Rear Seat Occupant Protection in Frontal Crashes and its Feasibility*. Enhanced Safety of Vehicles, 20th International Conference on the Enhanced Safety of Vehicles, Lyon, France, June 18-21, 2007.

[14] El-Jawahri, R. E., Kim A., Jaradi, D., Ruthinowski, R., Siasoco, K., Stancato, C. and Weerappuli, P. (2017). *Responses of Rear Seat ATDs in Frontal Impact Sled Tests: Evaluation of Two Seat Belt Configurations*. SAE International, SAE Technical Papers, 2SAE World Congress Experience, April 4-6, 2017.

[15] Forman, J., Michaelson, J., Kent, R., Kuppa, S., and Bostrom, O. (2008). *Occupant Restraint in the Rear Seat: ATD Responses to Standard and Pre-tensioning, Force-Limiting Belt Restraints*. Association for the Advancement of Automotive Medicine, Annals of Advances in Automotive Medicine: 52nd AAAM Annual Conference, October 2008.

[16] Hong, L., Yuhao, P., and Hongtao, X. (2018). *Research on the Safety of Rear Seat Female Occupant in the 50km/h Frontal Collision*. Institute of Physics Publishing, Journal of Physics: Conference Series, 1st

International Conference on Advanced Algorithms and Control Engineering, v 1087, n 5, ICAACE 2018, August 10-12, 2018.

[17] Hong, L. and Wu, Y. (2012). *Research on the Safety of Rear Seat Occupants in the Frontal Collision*. Trans Tech Publications, Advanced Materials Research, 569, 795-799.

[18] Hong, L., Ge, R., and Wu, Y. (2013). *Analysis and Optimization of Rear Occupant Safety in Car Head-On Collision*. Trans Tech Publications Ltd, Applied Mechanics and Materials, 328, 292-296.

[19] Tylko, S., and Bussieres, A. (2012). *Responses of the Hybrid III 5th Female and 10-year-old ATD Seated in the Rear Seats of Passenger Vehicles in Frontal Crash Tests*. International Research Council on the Biomechanics of Injury, 2012 IRCOBI Conference Proceedings, September 12-14, Paper No. IRC-12-65.

[20] Prasad, A. K. (2010). *Rear Seat Study*. SAE, Vehicle Research and Test Center NHTSA.

[21] Jakobsson, L., et al. (2019). *Rear Seat Safety in Frontal to Side Impacts – Focusing on Occupants from 3 Years to Small Adults.* Paper No. 11-0257.

[22] Hu, J., Fischer, K., Lange, P., and Adler, A. (2015). *Effects of Crash Pulse, Impact Angle, Occupant Size, Front Seat Location, and Restraint System on Rear Seat Occupant Protection*. SAE International, SAE Technical Papers, SAE 2015 World Congress and Exhibition, April 21-23, 2015.

[23] Tavakoli, M., and Brelin-Fornari, J. (2015). *Effects of Pretensioners and Load Limiters on 50th Male and 5th Female Seated in Rear Seat During a Frontal Collision*. SAE International, SAE Technical Papers, SAE 2015 World Congress and Exhibition, April 21-23, 2015.

[24] Forman, J., Lopez-Valdes, F., Lessley, D., Kindig, M., Kent, R., Ridella, S., and Bostrom, O. (2009). *Rear Seat Occupant Safety: An Investigation of a Progressive Force-Limiting, Pre-tensioning 3-Point Belt System Using Adult PMHS in Frontal Sled Tests.* SAE International, SAE Technical Papers, 2009-November, 53rd Stapp Car Crash Conference, November 2-4, 2009.

[25] Forman, J., Michaelson, J., Kent, R., Kuppa, S., and Bolstrom, O. (2008). *Occupant Restraint in the Rear Seat: ATD Responses to Standard and Pre-tensioning, Force-Limiting Belt Restraints*. Association for the Advancement of Automotive Medicine, Annals of Advances in Automotive Medicine: 52nd Annual Scientific Conference, October 6-8, 2008, 52, 141-153.

[26] Kent, R., Forman, J. Parent, D., and Kuppa, S. (2007). *The Feasibility and Effectiveness of Belt Pre-tensioning and Load Limiting for Adults in the Rear Seat*. Inderscience Enterprises Ltd, International Journal of Vehicle Safety, 2(4), 378-403.

[27] Michaelson, J., Forman, J. Kent, R. and Kuppa, S. (2008). *Rear Seat Occupant Safety: Kinematics and Injury of PMHS Restrained by a Standard 3-Point Belt in Frontal Crashes*. SAE International, SAE Technical Papers, 52nd Stapp Car Crash Conference, November 3-5, 2008.

[28] Bilston, L. E., Du, W., and Brown, J. (2010, November) *A Matched-Cohort Analysis of Belted Front and Rear Seat Occupants in Newer and Older Model Vehicles Shows That Gains in Front Occupant Safety Have Outpaced Gains for Rear Seat Occupants*. Elsevier Ltd, Accident Analysis and Prevention, 42(6), 1974-1977.

[29] Forman, J., Lopez-Valdes, F., Dennis, N., Kent, R., Tanji, H. and Higuchi, K. (2010). *An Inflatable Belt System in the Rear Seat Occupant Environment: Investigating Feasibility and Benefit in Frontal Impact Sled Tests with 50th Percentile Male ATD.* Association for the Advancement of Automotive Medicine, Annals of Advancement in Automotive Medicine: 54th Annual Scientific Conference, Las Vegas, Nevada, October 17-20, 2010, 111-125.

[30] Hesseling, R. J., Steinbuch, M. Veldpaus, F. E. and Klisch, T. (2002). *Control Design of a Safety Restraint System.* ASCC, The 4th Asian Control Conference, Singapore, September 25-27, 2002, 244-249.

[31] Gierczycka-Zbrozek, D. (2011). *Adaptive Restraints: Suggested Parameters for Occupant Classification System*. International Research Council on the Biomechanics of Injury, 2011 IRCOBI Conference Proceedings, 311-314. Paper No. IRC-11-74.

[32] Holding, P. N., Chinn, B. P., Happian-Smith, J. (2001). *An Evaluation of the Benefits of Active Restraint Systems in Frontal Impacts Through Computer Modeling and Dynamic Testing*. TRL Limited, Paper 328.

[33] Untaroiu, C. D. and Adam, T. (2012). *Occupant Classification for an Adaptive Restraint System: The Methodology and Benefits in Terms of Injury Reduction*. International Research Council on the Biomechanics of Injury, 2012 IRCOBI Conference Proceedings, September 12-14, 2012, 205-216. Paper No. IRC-12-28.

[34] Mroz, K., Pipkorn, B., Sunnevang, C., Eggers, A. and Brase, D. (2018). *Evaluation of Adaptive Belt Restraint Systems for the Protection of Elderly Occupants in Frontal Impacts*. International Research Council on the Biomechanics of Injury, 2018 IRCOBI Conference Proceedings, 60-75. Paper No. IRC-18-15.

[35] United States Code of Federal Regulations, Title 49, Subtitle B, Chapter V, §571.209, Federal Motor Vehicle Safety Standard No. 209; Seat belt assemblies.

[36] Goertz, A., Yaek, J., Compton, C. (2010). *Accident Statistical Distributions from NASS CDS.* Society of Automotive Engineers, Publication 2010-01-0139.

[37] MADYMO Software, Version 7.6, Release date : 14:01:49 Aug 31 2015, Copyright 2015, TASS International, Rijswijk, The Netherlands.

APPENDIX A – Vehicle crash pulses

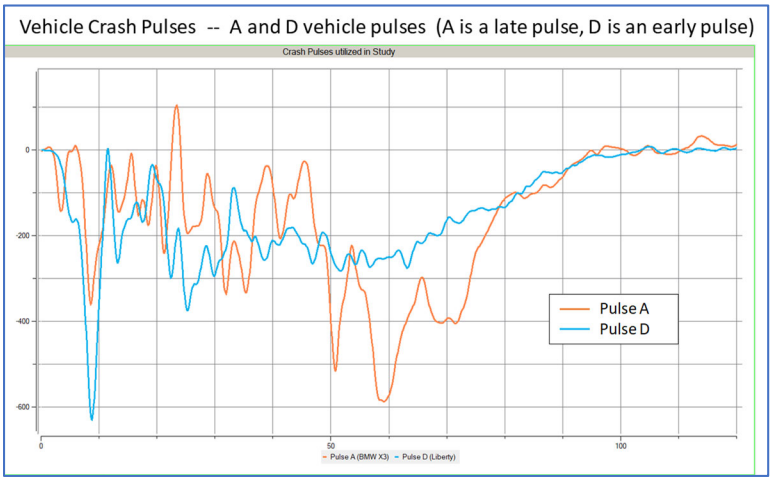

(a)

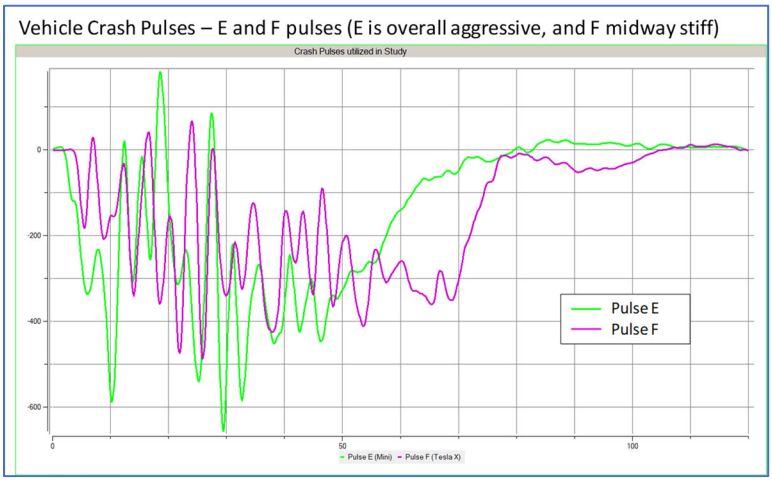

(b)

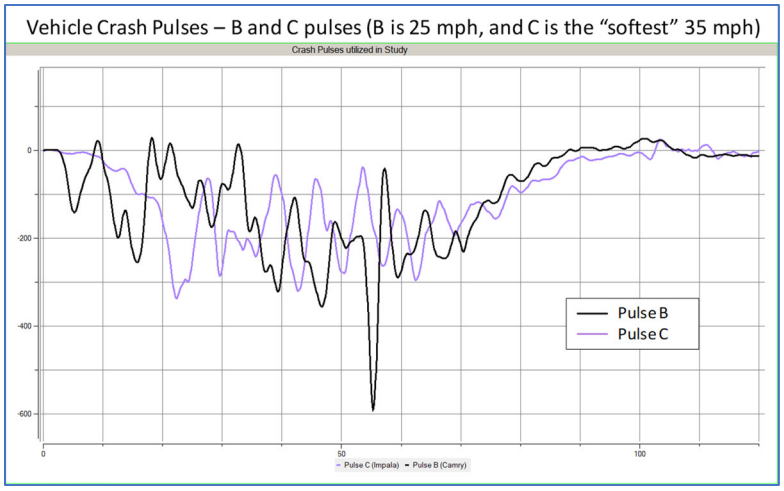

(c)

Figure A1. Overlays of the six simulation crash pulses (2 per graph).

APPENDIX B – Belt Pay-out amounts clustered per restraint technology

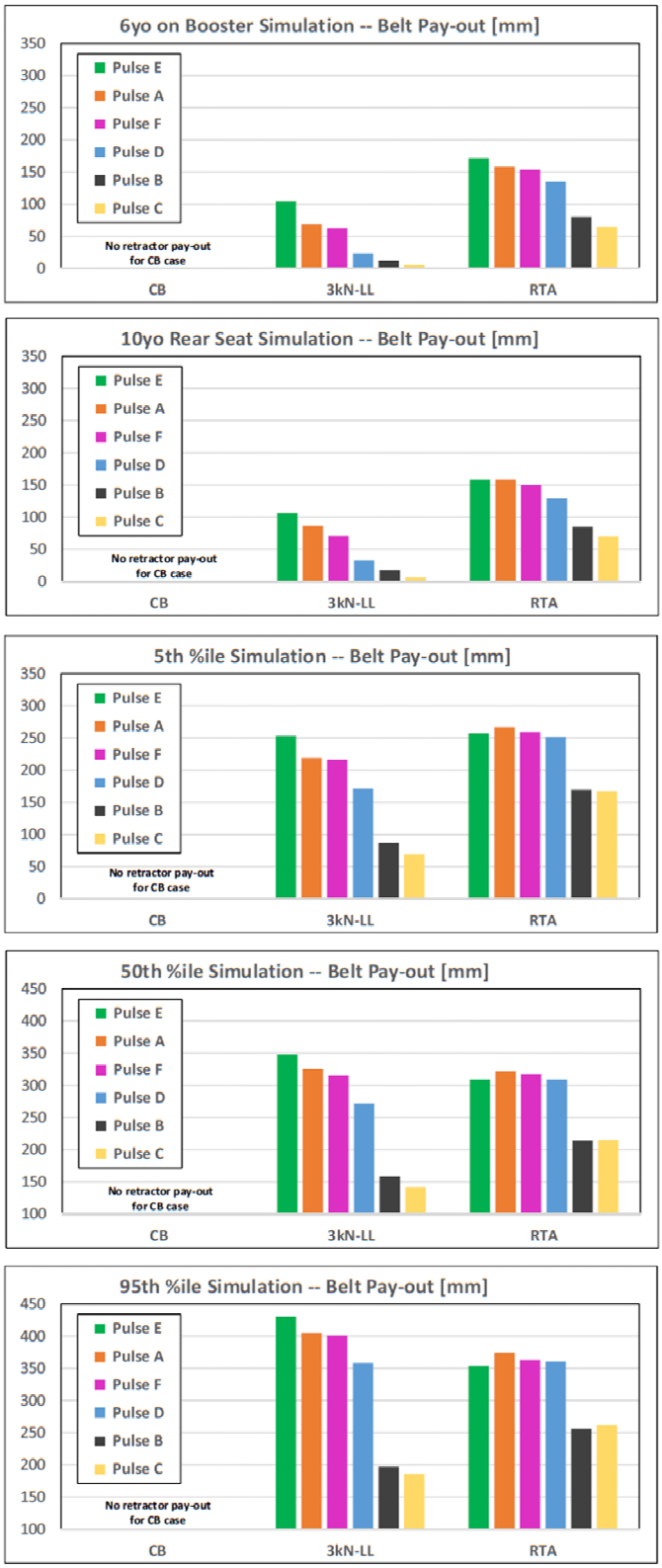

Figure B1. Simulation results – seatbelt pay-out amounts.

APPENDIX C – Shoulder belt seatbelt loads

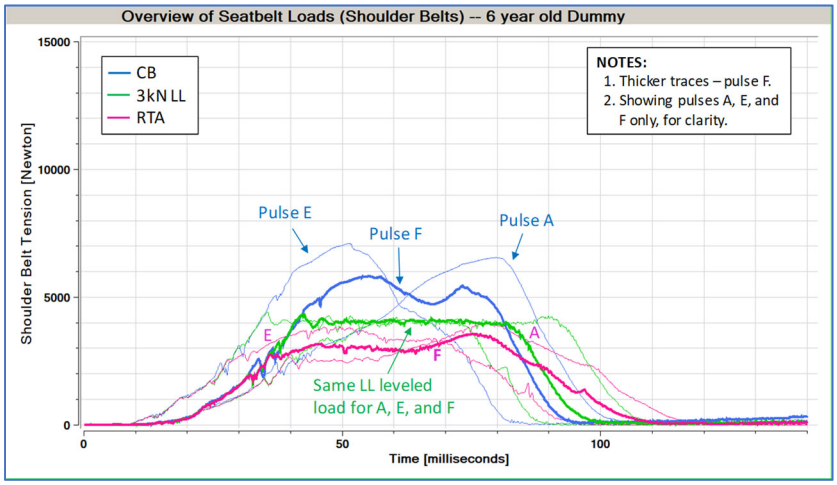

(a) HIII 6YO shoulder belt results.

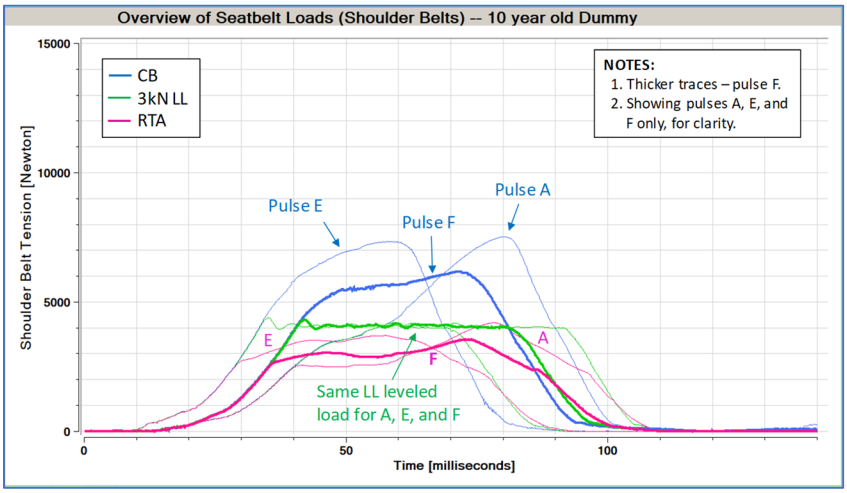

(b) Q10 shoulder belt results.

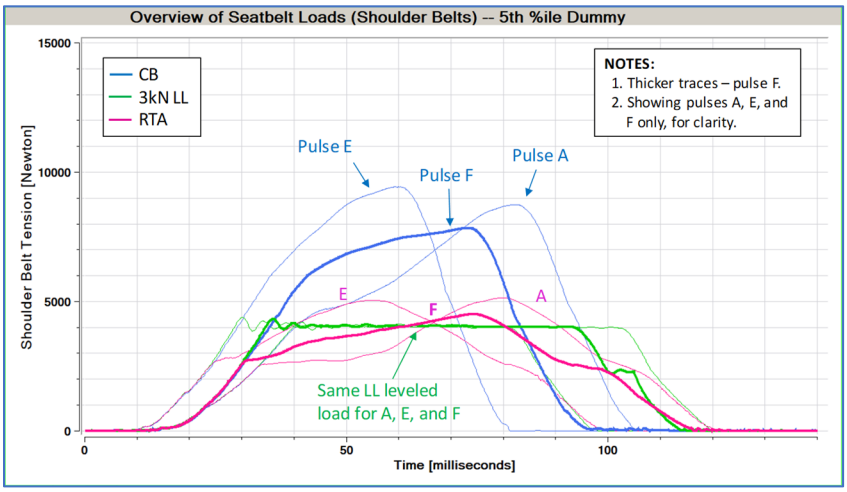

(c) HIII 5th percentile shoulder belt results.

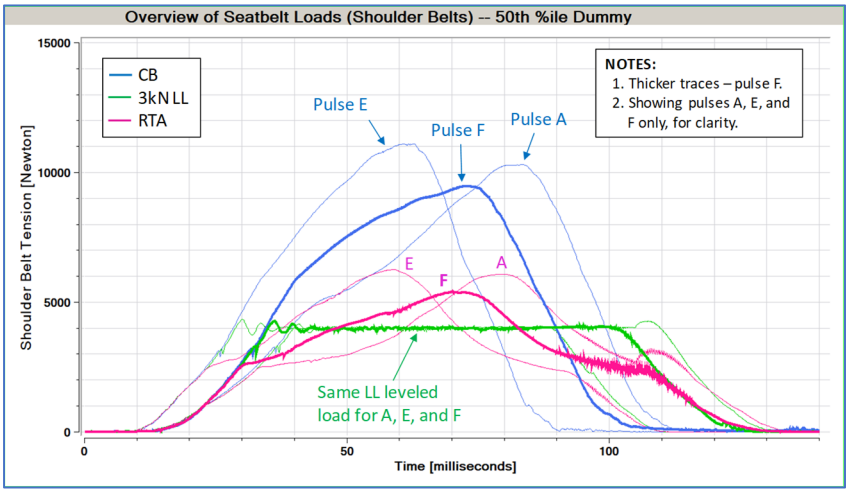

(d) HIII 50th percentile shoulder belt results.

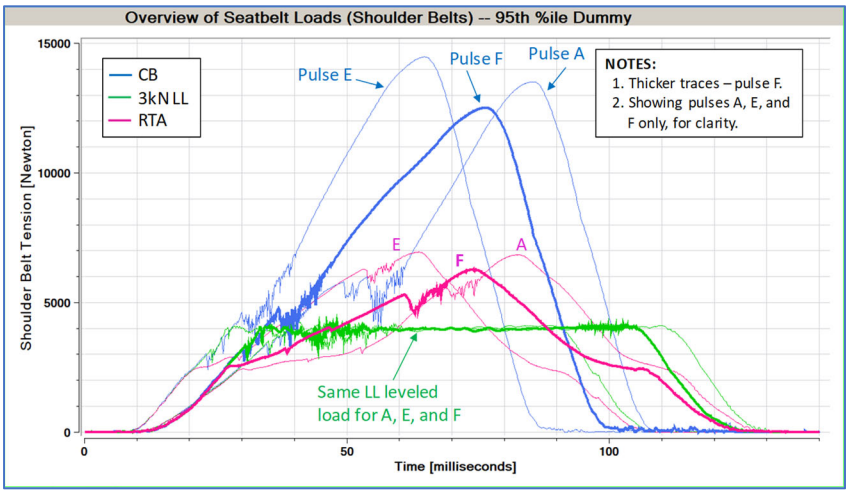

(e) HIII 95th percentile shoulder belt results.

Figure C1. Simulation results – shoulder belt loads.

APPENDIX D – Sample MADYMO Control System syntax

```
BELT                          ID=1 NAME=D-ringBelt
BELT                          ID=2 NAME=BuckleBelt
BELT                          ID=3 NAME=AnchorBelt
SENSOR.JOINT                  ID=2 NAME=Vehicle_sen_accel JOINT=../Vehicle_sys/joint_1
SENSOR.JOINT                  ID=3 NAME=Vehicle_sen_vel JOINT=../Vehicle_sys/joint_1
SENSOR.JOINT                  ID=21 NAME=LL_pos_sen JOINT=Retractor_trans_jnt
SENSOR.JOINT                  ID=22 NAME=LL_rate_sen JOINT=Retractor_trans_jnt
SENSOR.JOINT                  ID=23 NAME=Time_sens JOINT=../Time_tracker/Time_tracker_jnt
CONTROL_SYSTEM                ID=20 NAME=Value_6000_control
CONTROL_SYSTEM                ID=12 NAME=RateRefValue_15_control
CONTROL_SYSTEM                ID=11 NAME=Value_800_control
CONTROL_SYSTEM                ID=9 NAME=Value_1_control
CONTROL_SYSTEM                ID=6 NAME=Max_Payout_control
CONTROL_SYSTEM                ID=2 NAME=Nominal_3000_control
CONTROL_SYSTEM                ID=5 NAME=Max_Payout_to_Payout_control
CONTROL_SYSTEM                ID=7 NAME=Invert01_control
CONTROL_SYSTEM                ID=13 NAME=Invert02_control
CONTROL_SYSTEM                ID=8 NAME=Factor01_control
CONTROL_SYSTEM                ID=14 NAME=Factor02_control
CONTROL_SYSTEM                ID=15 NAME=Square01_control
CONTROL_SYSTEM                ID=16 NAME=Sum_of_1mRateWeight_control
CONTROL_SYSTEM                ID=10 NAME=One_minus_factor01_control
CONTROL_SYSTEM                ID=4 NAME=RateWeight01_control
CONTROL_SYSTEM                ID=1 NAME=LL_Mult01_control
CONTROL_SYSTEM                ID=3 NAME=Sum01_control
CONTROL_SYSTEM                ID=21 NAME=D_Seg01_control
CONTROL_SYSTEM                ID=17 NAME=RateWeight_mult_control
CONTROL_SYSTEM                ID=18 NAME=Min_control
CONTROL_SYSTEM                ID=19 NAME=Max_control
ACTUATOR.JOINT_POS            ID=1 NAME=Actuation01 JOINT=Retractor_trans_jnt
STATE.JOINT
SWITCH.LOGIC                  ID=15 NAME=No_reverse
SWITCH.TIME                   ID=14 NAME=Retractor_lock_called
OUTPUT_JOINT_DOF              ID=1 NAME=Belt_pay-out
OUTPUT_JOINT_DOF              ID=2 NAME=Belt_pay-out_rate
OUTPUT_JOINT_CONSTRAINT       ID=1 NAME=Retractor_trans_force JOINT=Retractor_trans_jnt
```

Figure D1. Sample MADYMO Control System syntax for RTA model.

APPENDIX E – TCJ Technology Reference Information

The Tailored Control Joint (or TCJ) Technology is a mechatronic system designed specifically for adaptive load control applications in the translational or rotational modes, and for clutch applications. Development and prototyping efforts currently occur at BGM Engineering, Shelby Township, MI, USA. Established patent rights (US Patent #6,384,518) and Patent Pending rights apply.

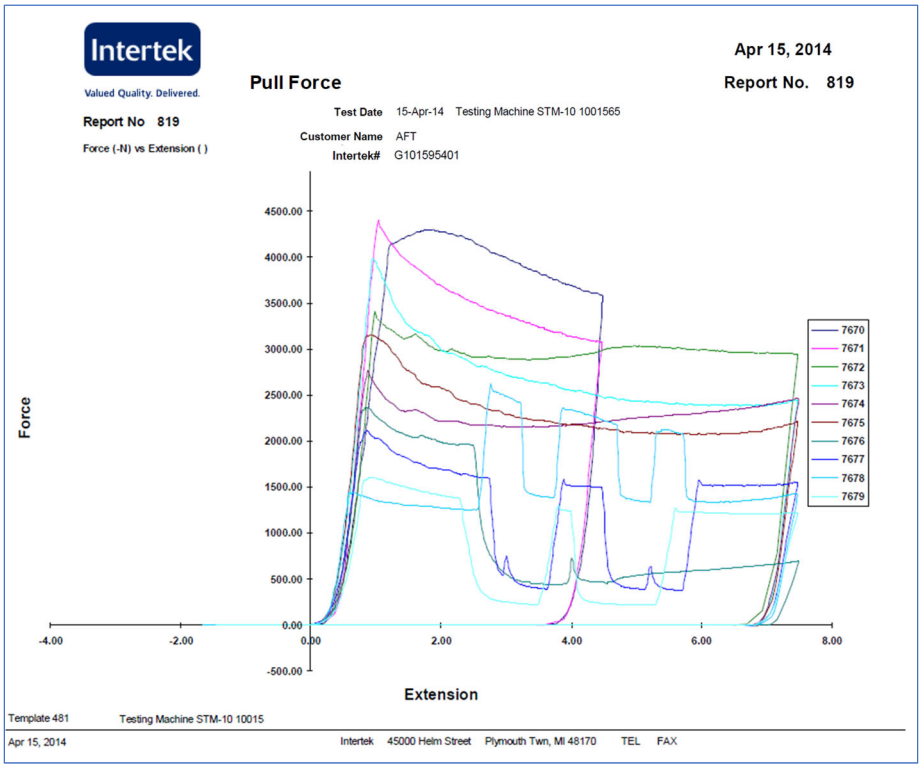

Figure E1. Sample TCJ technology test data conducted at Intertek, Plymouth, MI, USA.

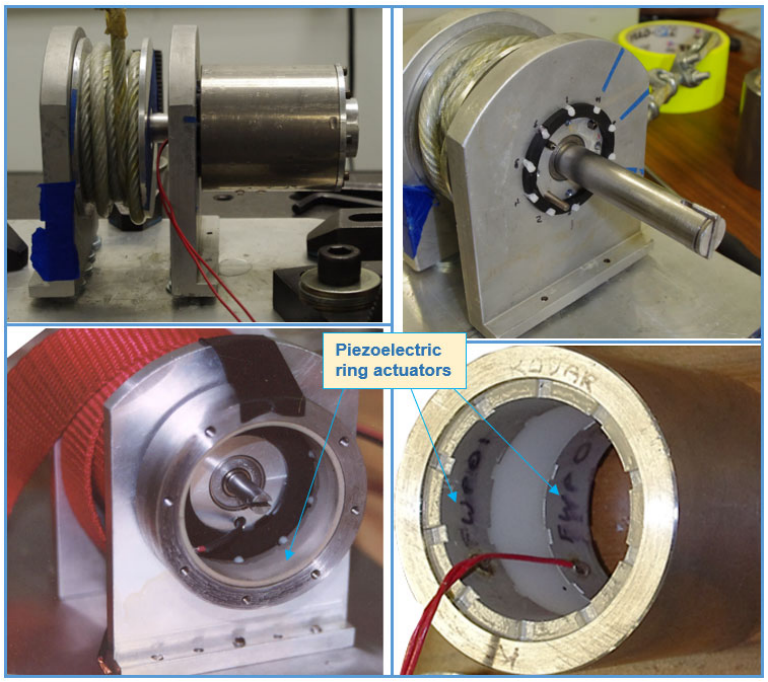

Figure E2. Sample TCJ technology prototypes and components.